

**NEW THEORY OF EFFECTIVE WORK FUNCTIONS AT METAL/HIGH-K
DIELECTRIC INTERFACES
-APPLICATION TO METAL/HIGH-K HfO₂ and La₂O₃ DIELECTRIC
INTERFACES -**

Kenji Shiraishi^{1,2}, Takashi Nakayama³, Yasushi Akasaka⁴, Seiichi Miyazaki^{5,2},
Takashi Nakaoka¹, Kenji Ohmori², Parhat Ahmet⁶, Kazuyoshi Torii^{4,9}, Heiji Watanabe^{7,2},
Toyohiro Chikyow², Yasuo Nara⁴, Hiroshi Iwai⁶, and Keisaku Yamada^{8,2}

¹Graduate School of Pure and Applied Sciences, University of Tsukuba,
1-1-1 Tennodai, Tsukuba, Ibaraki 305-8571 Japan

²National Institute for Material Science, 1-1 Namiki, Tsukuba, Ibaraki 305-0044 Japan

³Department of Physics, Faculty of Science, Chiba University,
1-33 Yayoi-cho, Inage-ku, Chiba, 263-8522 Japan

⁴Semiconductor Leading Edge Technologies inc.,
16-1 Onogawa, Tsukuba, Ibaraki 305-8569 Japan

⁵Graduate School of Advanced Sciences of Matter, Hiroshima University,
1-3-1 Kagamiyama, Higashi-Hiroshima, Hiroshima 738-8530, Japan

⁶Frontier Collaborative Research Center, Tokyo Institute of Technology,
4259 Nagatsuta, Midori-ku, Yokohama, Kanagawa, 226-8502, Japan

⁷Graduate School of Engineering, Osaka University,
2-1 Yamada-oka, Suita, Osaka 565-0871, Japan

⁸Nanotechnology Research Laboratory, Waseda University,
513 Waseda Tsurumaki-cho, Shinjuku-ku, Tokyo 169-0041 Japan.

⁹Present Address: Central Research Laboratory, Hitachi Ltd.,
1-280 Higashi-koigakubo, Kokubunji, Tokyo 185-8601 Japan

Abstract

We have constructed a universal theory of the work functions at metal/high-k HfO₂ and La₂O₃ dielectric interfaces by introducing a new concept of generalized charge neutrality levels. Our theory systematically reproduces the experimentally observed work functions of various gate metals on Hf-based high-k dielectrics, including the hitherto unpredictable behaviors of the work functions of *p*-metals. Our new concept provides effective guiding principles to achieving near-band-edge work functions of gate metals. Moreover, we discuss the potential of the new high-k dielectrics of La₂O₃ based on this new concept.

INTRODUCTION

The considerable downscaling of Si devices has brought about the requirement for a continuing need for significant reduction in gate dielectric film thickness; even current commercially based large scale integrated (LSI) circuits have SiO₂ dielectrics of ~15 Å thickness. As a result, the increasing gate leakage current has become a serious issue for future LSI devices. Efforts to reduce the leakage current have given rise to the application of alternative high-*k* gate dielectrics, which have been and still are being studied intensively. HfO₂ related high-k dielectrics have attracted much attention because of their desirable properties, such as the thermal stabilities when they are in contact with Si, and they are expected to be used for 45-nm node devices (1, 2). Furthermore, La₂O₃ related

high-k dielectrics are potential candidates for the 32-nm node devices and beyond (3). In addition to high-k dielectrics, for the 45-nm node devices and beyond, metal gates are also necessary in order to avoid the gate depletion effects.

Although high-k gate dielectrics with metal gates are being intensively studied, many obstacles still remain. One of them is the difficulty in controlling the effective work function (WF) of the gate metal. The effective WFs of gate metals on Hf-based high-k dielectrics reveal unexpected behaviors that are much different from those both in vacuum and on SiO₂: (a) It is reported that the WFs of *p*-metals such as Au and Pt increase on Hf-based dielectrics and resulting in slope parameters larger than unity (4). (b) The WFs of NiSi and Ni₃Si are different on HfSiON, although both their WFs in vacuum and on SiO₂ are almost the same (5). These phenomena cannot be explained by the existing models such as Hf-Si bond model (6) nor the conventional charge neutrality level concept (7-9). On the other hand, it is doubtless that oxygen vacancies (Vo) exert crucial effects on the WFs of gate materials; they cause Fermi level pinning (FLP) in poly-Si gates (10-12) and an O₂ pressure induced instability of *p*-metal WFs (13). In this paper, we have found by the first principles calculations that the conventional charge neutrality level concept cannot be applied to metal/high-k dielectric interfaces, since the assumptions that are necessary for the derivation of the conventional charge neutrality level concept are not satisfied in these systems. This means that the development of a new concept is needed to enable us to predict the effective WFs at metal/high-k interfaces.

In this paper, we propose a new theory to determine the effective WF at metal/high-k dielectric interfaces. We introduce a new concept of a generalized charge neutrality level, $\phi(\text{GCNL})$, and show that both $\phi(\text{GCNL})$ and Vo effects play crucial roles in determining the effective WFs of metals on high-k dielectrics (14). Based on the proposed theory, we have succeeded in reproducing and predicting the hitherto unpredictable behavior of the WFs of metals on Hf-related high-k dielectrics. A useful guiding principle for gate metal selection is presented based on our proposed theory. Moreover, we also consider the usefulness of a new high-k gate dielectric, La₂O₃, using our proposed guiding principle.

CONVENTIONAL CHARGE NEUTRALITY LEVEL CONCEPT

Hetero-interfaces including metal/insulator interfaces have been enthusiastically studied for a long period of time, both from the scientific and technological viewpoints. Interface physics is one of the most important fields of condensed matter physics, and important concepts were constructed in 1970s and 1980s. Among them, metal induced gap states (MIGS) (15) and the conventional charge neutrality level (10-12) are particularly important concepts, since they can give an insight into the effective WF at metal/insulator interfaces and the band offsets at hetero-semiconductor interfaces.

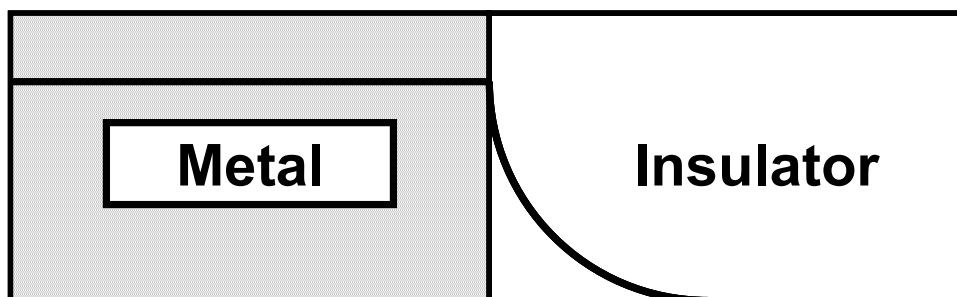


Fig.1: Schematic illustration of metal induced gap states (MIGS).

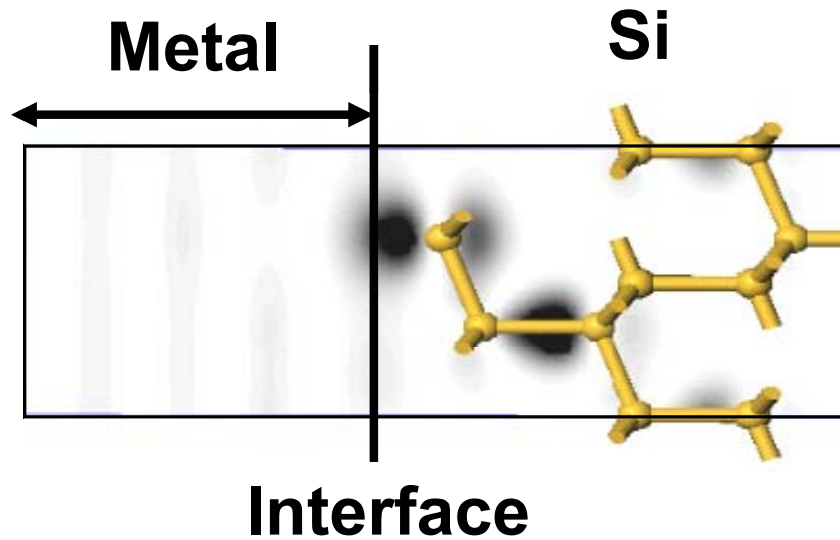


Fig.2: Contour plot of metal induced gap states (MIGS) at the metal/Si interfaces. The dark regions correspond to the large electron density regions.

We briefly mention the conventional charge neutrality level concept. Before explaining this, we will first give the basic physical background to MIGS. In the energy band gap of bulk insulators, there are no states. However, when a metal is in contact with an insulator, electronic states with amplitudes in the insulator region appear in the insulator band gap. These states are called as metal induced gap states (MIGS). MIGS wave functions generally have large amplitude in the metal region and decay inside the insulator as illustrated in Fig.1. This can be interpreted mathematically by the MIGS having an imaginary wave number k inside the insulator and decaying as e^{-kz} , similar to the wave functions in a potential barrier. In the case of a relatively small band gap material such as silicon, the MIGS penetration depth is relatively deep as shown in Fig. 2 (15). In 1984, Tersoff proposed the conventional charge neutrality level concept based on the two assumptions as illustrated in Fig. 3 (6).

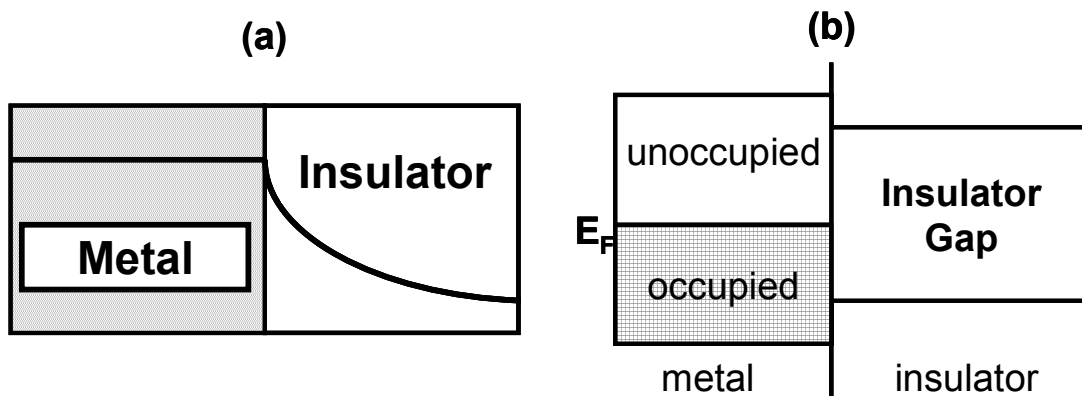


Fig.3: Schematic illustration of the two assumptions made when deriving the conventional charge neutrality level.

- (a) MIGS penetrate to a sufficient depth in an insulator.
- (b) The metal density of states (DOS) is almost constant.

Based on the above two assumptions, he constructed the concept of the conventional charge neutrality level. This level corresponds to the energy level at which a character of the MIGS wave function changes from acceptor-like to donor-like. A schematic illustration of the conventional charge neutrality level concept is given in Fig. 4. After the original work of Tersoff (7), Cardona and Christensen proposed a more convenient form of the charge neutrality level in 1987 (8). In their definition, the charge neutrality level can be determined by the weighted average of the conduction band DOS and the valence band DOS as follows.

$$\phi(\text{CNL}) = E_{\text{VB}} + E_g D_{\text{VB}} / (D_{\text{VB}} + D_{\text{CB}}), \quad [1]$$

where, E_g , E_{VB} , D_{VB} , and D_{CB} are the band gap, the valence band energy, and the DOS in the valence and conduction bands, respectively.

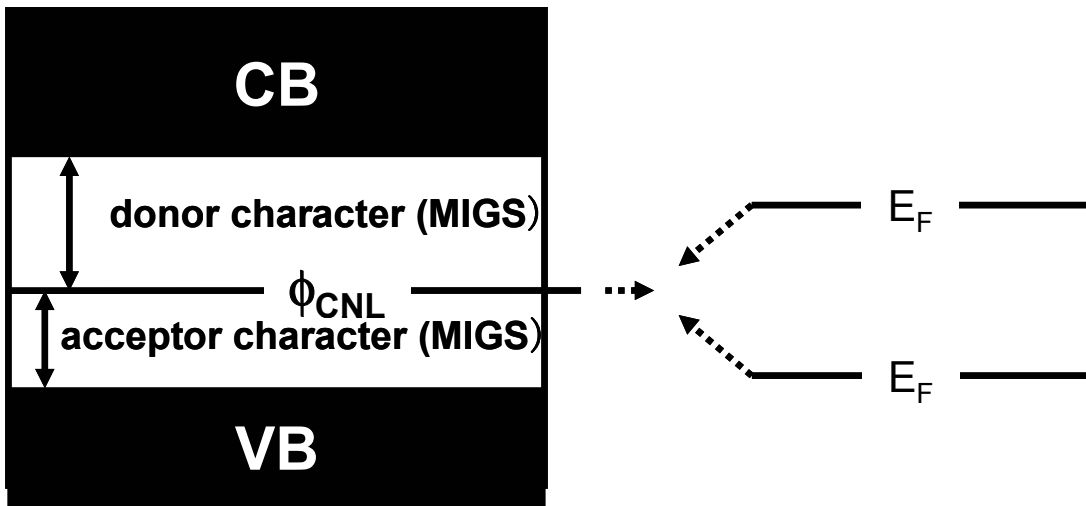


Fig.4: Schematic illustration of the basic concept of the conventional charge neutrality level.

Based on Eq. [1], many experimental results such as the Schottky barrier heights at metal/semiconductor interfaces and band offsets in semiconductor hetero structures, can be reproduced (7, 8). In the case of semiconductor hetero structures, the conventional charge neutrality concept works particularly well when the common anion rule is satisfied (7, 8). The common anion rule means that the interface can be defined by the same anion atoms such as in the AlAs/GaAs hetero interface shown in Fig. 5. Furthermore, Robertson has recently succeeded in reproducing the band offsets of various metal oxides (9). This is because the hetero oxide interface is the typical systems for which the common anion rule is satisfied.

In case of wide band gap materials such as insulators, however, it is well known that the Schottky barrier height (or effective WFs) at the metal/insulator interface does not match the conventional charge neutrality level. However, the effective WF of a metal generally tends to move towards the conventional charge neutrality levels but does not

reach it, as shown in Fig. 4. Thus, a semi-empirical parameter called the slope parameter (S) is introduced to analyze the effective WF at the metal/insulator interface (16). S is given by the following equation. It is noticeable that S should be in the range of $0 < S < 1$ according to the restriction caused by the conventional charge neutrality level concept.

$$S = \frac{\partial(\text{effective WF})}{\partial(\text{vacuum WF})}. \quad [2]$$

For metal/HfO₂ interfaces, there have been reports that the conventional charge neutrality concept with the slope parameter works well for relatively low work function metals (17).

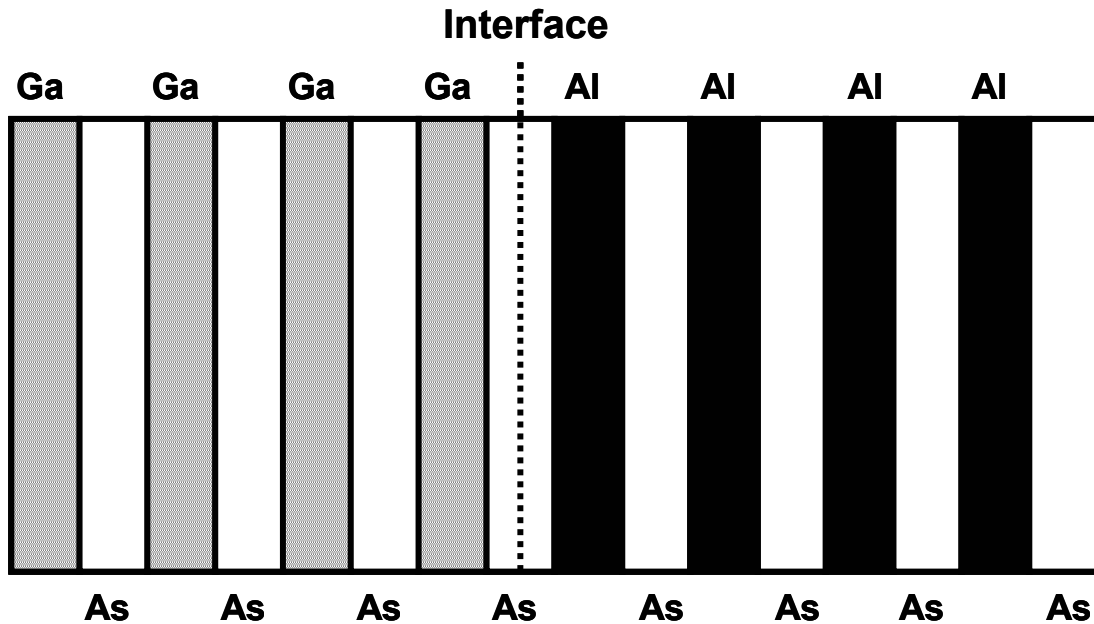


Fig.5: Schematic illustration of the GaAs/AlAs semiconductor hetero interface in which the common anion rule is satisfied.

A NEW CONCEPT OF THE GENERALIZED CHARGE NEUTRALITY LEVEL

As discussed in the previous sections, the conventional charge neutrality level has been widely accepted and it works well in analyzing the effective WFs of metal/insulator interfaces by introducing a slope parameter S. Very recently, however, the unexpected behaviors of metal effective WFs on Hf-related high-k gate dielectrics have been reported, especially in high work function metals (4, 5). For example, it was reported that the WFs of *p*-metals such as Au and Pt, increase on Hf-based dielectrics and the resulting slope parameters are larger than unity as shown in Fig. 6(a) (4). The fact that $S > 1$ is extraordinary result, since the conventional charge neutrality level concept only gives S values that are always smaller than unity. Moreover, it is also reported that effective WFs of NiSi and Ni₃Si are different on HfSiON, although both their WFs in vacuum and on SiO₂ are almost the same as shown in Fig. 6(b) (5). In short, recent several experimental reports show that the conventional charge neutrality level concept cannot explain the effective WFs at metal/Hf-based high-k dielectric interfaces.

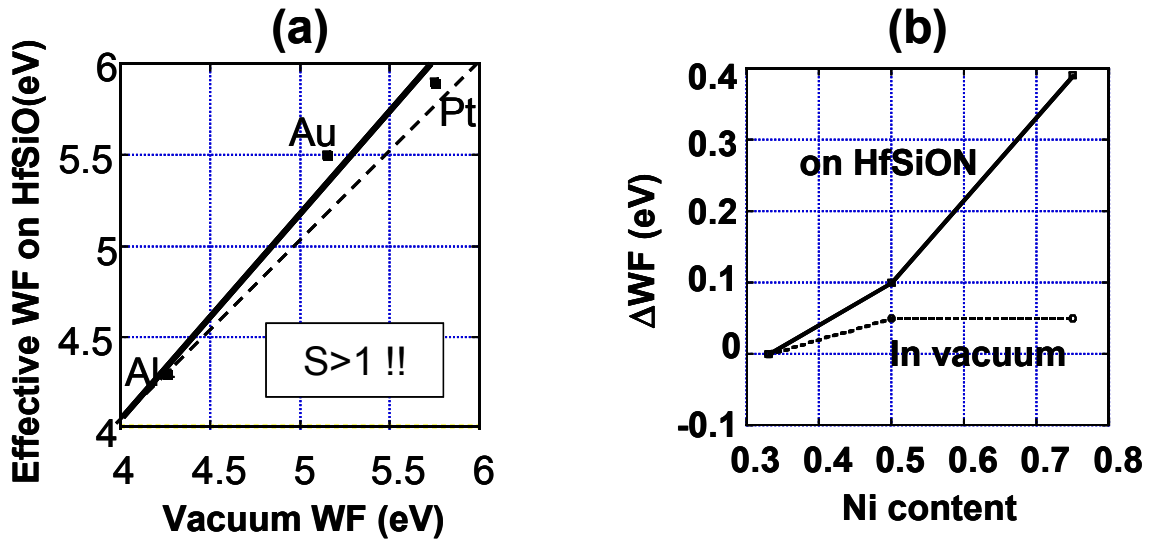


Fig.6: (a) Extracted WFs of Al, Au and Pt on HfSiON plotted as a function of the vacuum WFs reported in Ref [4]. The slope parameter (S) is larger than 1. (The broken line indicates the S=1 line). (b) Extracted WFs both on HfSiON and in vacuum as functions of Ni content in Ref [5].

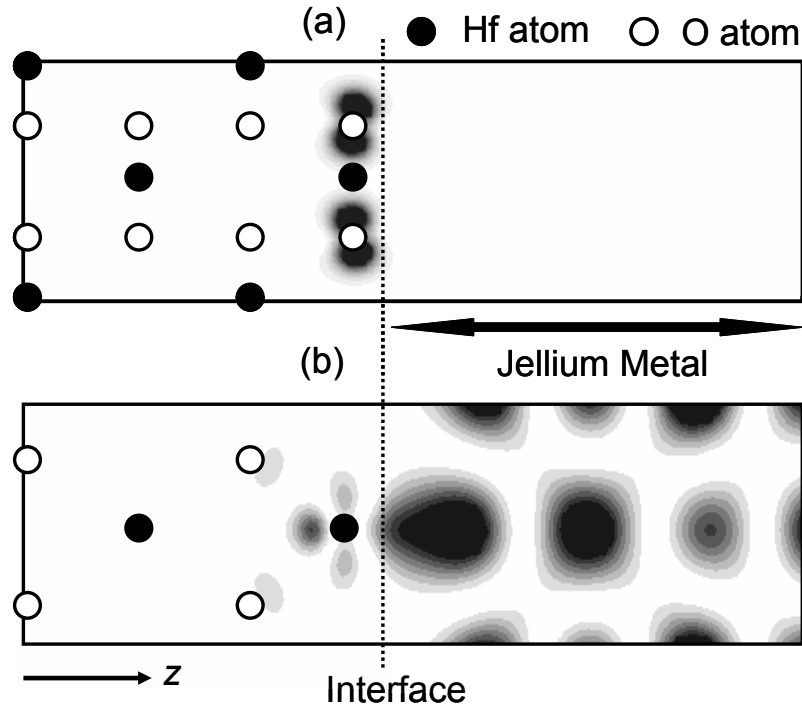


Fig.7: Contour plots of MIGS wave functions.(a) MIGS wave function with large amplitude at O atoms. (b) MIGS wave function with large amplitude at Hf atoms.

In order to clarify the failure of the conventional charge neutrality level concept to explain these results, we performed first principles calculations at metal/HfO₂ interfaces. First, we focused on the penetration depth of the metal induced gap states (MIGS), which

is related to the first assumption in the derivation of the conventional charge neutrality level. The calculations are based on the generalized gradient approximation (18), and ultrasoft pseudopotentials (19, 20). Pseudo wave functions are expanded by the plane wave basis set with a kinetic energy cut-off value of 36 Ry. In the present calculations, the metal is approximated by the simple jellium model in which the positive ions are uniformly distributed and structural optimization has not been performed. In the present study, we investigate the HfO₂(110) interface, which is the neutrally charged faces. The models used have super lattice structures and they consist of 24.9 Å jellium metal regions and 9 atomic layer thick HfO₂ regions. The electron density used for the jellium metal is the same as Al. For the distance between the jellium and the HfO₂ layer (d), we chose $d=2.54$ Å.

Figures 7(a) and (b) show two typical MIGS obtained in the present calculations. It is noticeable that the penetration depth of the MIGS into the HfO₂ is within 1~2 atomic layers. The small penetration depth of the MIGS means that the first assumption of the conventional charge neutrality level concept is not satisfied. This reflects the large band gap of HfO₂. A characteristic feature of the MIGS at a jellium/HfO₂ interface is that the MIGS have large amplitudes at both the cation (Hf) and the anion (O); Figure 7(a) shows a typical example of MIGS with a large amplitude at the O atoms, and Fig. 7(b) describes MIGS with a large amplitude at the Hf atoms. These results indicate that metal wave functions can strongly hybridize with Hf 5*d* orbitals at the metal/HfO₂ interfaces, although the Hf⁴⁺ ion radius (0.8 Å) is much smaller than the O²⁻ ion radius (1.4 Å). Large hybridization with Hf 5*d* orbitals can be explained as follows. In Fig.8, the atomic wave functions of the Hf 5*d* and O 2*p* orbitals are shown. As described in this figure, empty Hf 5*d* orbital spreads to the outermost region. This delocalized feature of the Hf 5*d* orbital is the cause of its large hybridization with metal wave functions. As discussed above, the MIGS at the metal/HfO₂ interface penetrate very slightly into the HfO₂ region, and Hf 5*d* orbital can strongly hybridize with the metals due to its delocalized features [21].

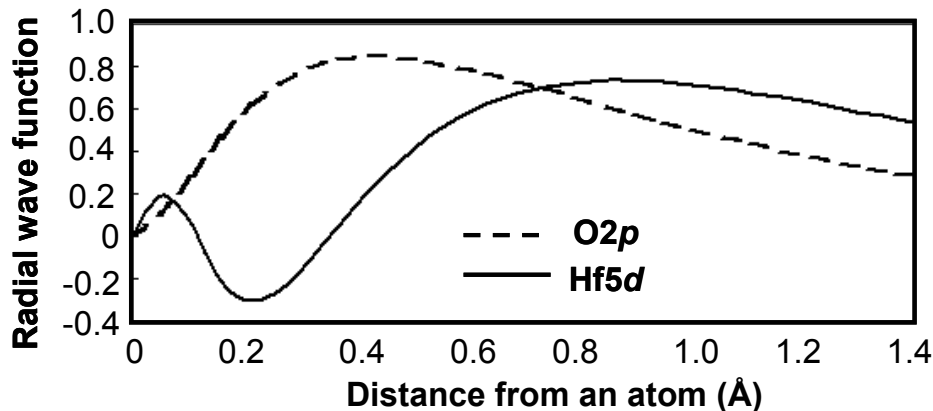


Fig.8: Atomic wave functions of Hf 5*d* and O 2*p* orbitals.

Next, we examine the second assumption used in deriving the conventional charge neutrality level concept, that the metal density of states (DOS) is almost constant. In Fig.9, we show the band structures of typical metals; Al, Au and Ni. As shown in these figures, the occupied DOS is much larger than the unoccupied DOS in the typical *p*-metals, Au and Ni, because of the existence of the narrow and dense *d*-bands just below the Fermi

level. Therefore, the second assumption that the metal density of state is almost constant is not satisfied in *p*-metals such as Au and Ni.

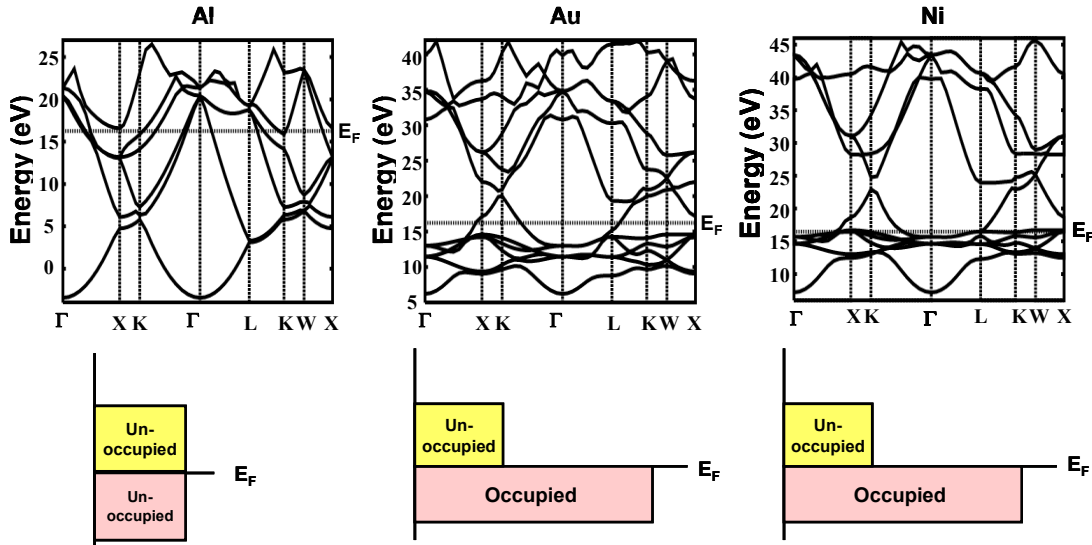


Fig.9: Bulk band structures and corresponding schematic density of states (DOS) of typical metals (Al, Au, and Ni) obtained by the first principles calculations.

The fact that the two major assumptions of the conventional charge neutrality level concept are not satisfied at the metal/ HfO_2 interface indicates that a new theoretical framework is necessary for considering metal/high-*k* dielectric interfaces. In developing a new concept, we take note of the fact that the MIGS penetration depth is only 1 or 2 atomic layers. We only take into account the electron transfer induced by the hybridization of atomic orbitals at the interface and determine the charge neutrality condition. The relationship between hybridization at the interface and the electron transfer direction is schematically shown in Fig. 10. At metal/insulator interfaces, there are four types of interface hybridization as follows.

- (a) Interface hybridization between metal occupied states and insulator valence bands.
- (b) Interface hybridization between metal unoccupied states and insulator conduction bands.
- (c) Interface hybridization between metal occupied states and insulator conduction bands.
- (d) Interface hybridization between metal unoccupied states and insulator valence bands.

We explain the above four types of hybridizations at the interface and their induced electron transfers.

- (a) For the interface hybridization between metal occupied states and insulator valence bands, both bonding and anti-bonding states are occupied after hybridization as shown in Fig. 10 (a). This means that no net electron transfer occurs by this hybridization.
- (b) For the interface hybridization between metal unoccupied states and insulator conduction bands, both bonding and anti-bonding states are unoccupied after hybridization as shown in Fig. 10 (b). As a result, this hybridization does not induce interface electron transfer.

- (c) For the interface hybridization between metal occupied states and insulator conduction bands, only the bonding state is occupied by two electrons. The bonding state wave function is mainly composed of the metal occupied state wave function. However, it also contains small amount of the insulator conduction band wave function due to the hybridization, as shown in Fig. 10 (c). This corresponds to an effective electron transfer from the metal to the insulator.
- (d) In the case of interface hybridization between metal unoccupied states and insulator valence bands, only the bonding state is occupied by two electrons. Although the bonding state wave function mainly consists of the insulator valence band wave function, it contains a small amount of the metal unoccupied state wave function as a result of the hybridization, as shown in Fig. 10 (d). This leads to an effective electron transfer from the insulator to the metal.

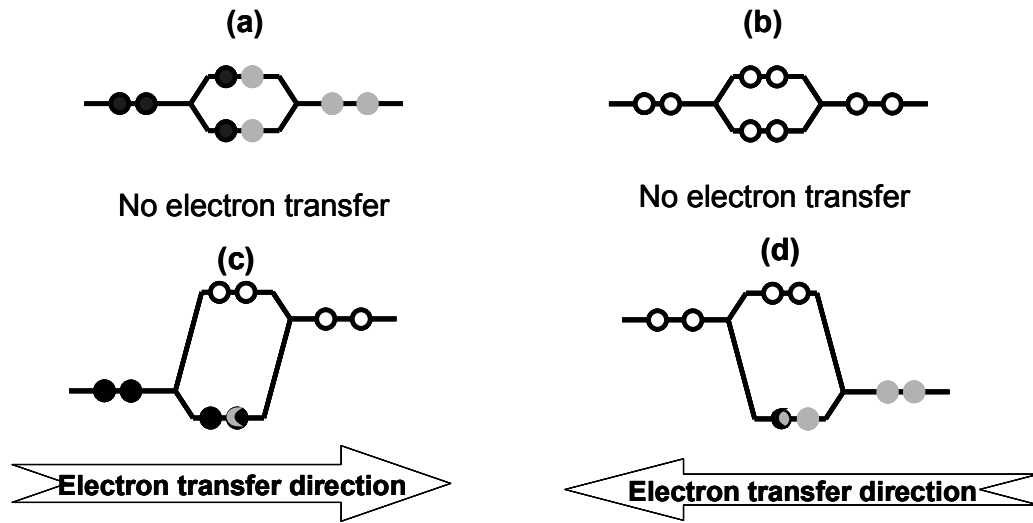


Fig.10: Schematic illustration of the relationship between hybridizations at the interfaces and the electron transfer directions.

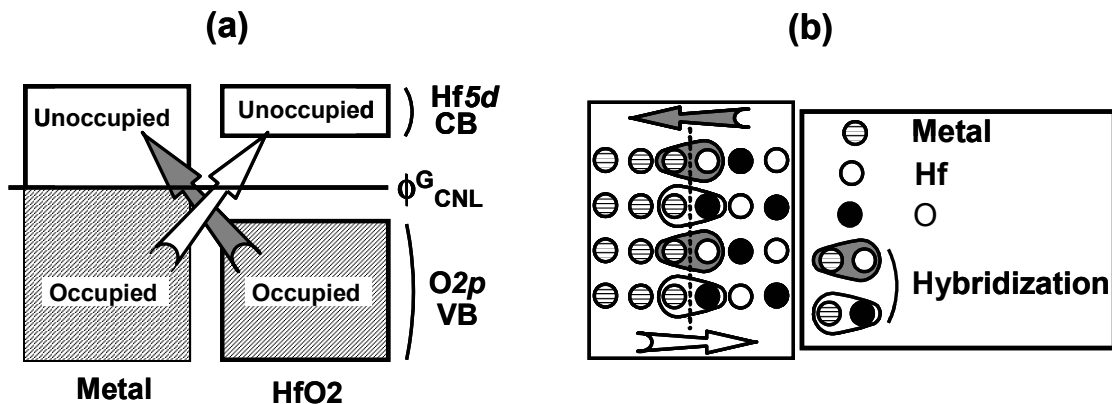


Fig.11: Schematic illustration of the $\phi(\text{GCNL})$ concept. (a) At $\phi(\text{GCNL})$, the metal-O and metal-Hf hybridizations, which induce interface electron transfer from HfO_2 to metal and metal to HfO_2 , are balanced and the net electron transfer is zero. (b) Atomistic illustration of the balanced situation of interface dipoles induced by interface metal-O and metal-Hf hybridization at an energy of $\phi(\text{GCNL})$.

As discussed above, interface electron transfer is induced by two types of hybridizations at the interfaces; (c) Hybridization between metal occupied states and insulator conduction bands (electron transfer from the metal to the insulator) and (d) Hybridization between metal unoccupied states and insulator valence bands (electron transfer from the insulator to the metal). Therefore, the charge neutrality condition is determined by the condition that the net electron transfer induced by hybridization at the interface is zero. We call the energy level that satisfies the above charge neutrality condition the “generalized charge neutrality level” $\phi(\text{GCNL})$. In Fig. 11, a schematic illustration of the concept of the generalized charge neutrality level, $\phi(\text{GCNL})$, at a metal/HfO₂ interface is described.

Since a high-k metal oxide is generally an ionic material, the main conduction band and valence band characters are metal cations (M) and O-2*p* atomic orbitals, respectively. Thus, we approximate the conduction band and valence band characters of high-k metal oxides by a linear combination of metal cations (M) and O atomic orbitals, respectively. This approximation is rather rough but it reflects the essential characteristics of an ionic high-k metal oxide. Furthermore, in the derivation of $\phi(\text{GCNL})$, we treat metal (m)-M and metal (m)-O hybridizations based on the second order perturbation theory. Metal wave functions are expressed by the Bloch form of the linear combination of atomic orbitals (LACO), and they can only hybridize with the M and O atomic orbitals close to the interface. Finally, $\phi(\text{GCNL})$ is expressed as

$$\phi(\text{GCNL}) = E_{VB} + \frac{E_g D_{unocc} N_O |t_{m-O}|^2}{D_{unocc} N_O |t_{m-O}|^2 + D_{occ} N_M |t_{m-M}|^2}. \quad [3]$$

The parameters in Eq.[3] are the m-M and m-O interactions (t_{m-M} , t_{m-O}), the DOS of the occupied and unoccupied states of the metals, (D_{occ} , D_{unocc}), the number of interfacial M and O atomic orbitals that can interact with metal wave functions, (N_M , N_O), the band gap and the valence band energy of the high-k metal oxide, (E_g , E_{VB}).

It is noticeable that the number of O and M orbitals that interact with metal wave functions (N_O , N_M), and the occupied and unoccupied DOS of the metal, (D_{occ} , D_{unocc}) are crucial in determining $\phi(\text{GCNL})$. This means that both the interface structures and the metal band structures are important for predicting the WFs at metal/high-k dielectric interfaces. There has been a report that the interface structure is very important in determining the band offset of semiconductor hetero-interfaces. Nakayama found by the first principles calculations that the calculated band offset values at ZnSe/GaAs interfaces change by about 1.0 eV, depending on whether the interface bonding is Zn-As or Se-Ga (22).

RESULTS AND DISCUSSIONS

Estimated $\phi(\text{GCNL})$ of a typical gate metal and experimental confirmation of the validity of our $\phi(\text{GCNL})$ theory in predicting n- and p-metal WFs on high-k HfO₂ gate dielectrics

To estimate $\phi(\text{GCNL})$ on HfO₂, we need information about the interface structure and the band structures of the metal as mentioned in the previous section. The interface structure can be predicted by considering the reactivity of the gate metal with O. In general, *n*-metal/HfO₂ interfaces mainly consist of metal-O-Hf bonds, whereas, *p*-metal/HfO₂ interfaces contain both metal-Hf and metal-O-Hf bonds. This prediction is based on the high and low reactivity of *n*- and *p*-metals, respectively, with O. As previously mentioned in Fig.9, the occupied DOS of Au and Ni are much larger than the

unoccupied DOS, whereas such DOS characteristics are not observed in Al. This effectively enhances the (Au(Ni)-*d*)-(Hf-5*d*) hybridization that causes electron transfer from metals to HfO₂, and $\phi(\text{GCNL})$ for Au(Ni) finally obtained is located in the lower part of the HfO₂ band gap. In contrast, $\phi(\text{GCNL})$ for Al is located in the upper part of the HfO₂ band gap because of the Al-O-Hf interface structures.

In Fig.12, we indicate the predicted interface structures of typical gate metals considering the reactivity with O. By taking into account both the interface structures and metal band structures, we obtain a rough estimate of $\phi(\text{GCNL})$ for typical metals. This is shown in Fig. 13. In the estimation, the interfacial bond number ratio $N_{\text{metal-Hf}}/N_{\text{metal-O-Hf}}$ is assumed to be 0 for *n*-metals and 0.5 for *p*-metals. We also include the second nearest neighbor interactions.

mainly M-O-Hf bonds	Si, Al, Ti, Zr, Ta TaN TaC
Both M-Hf and M-O-Hf bonds	Au, Ni, Pt, Re Ag, W, Ru

Fig. 12: Schematic illustration of the interfaces of typical gate metals and Hf-based high-k dielectrics. The interface structures are those expected from the metal reactivity with O. For Al and Ni, the present estimations are in good agreement with the first principles calculations.

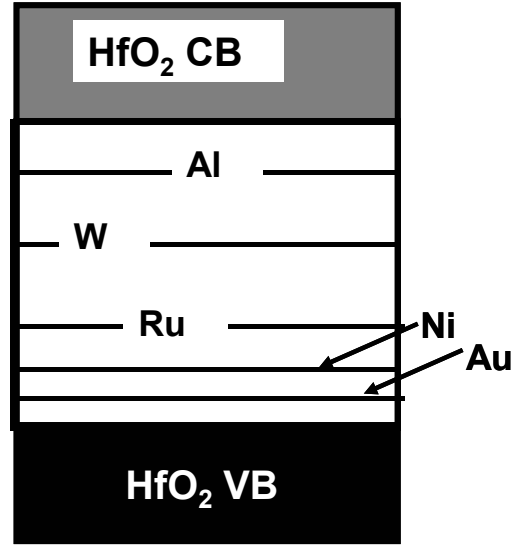


Fig.13: Rough estimate of $\phi(\text{GCNL})$ for typical gate metals.

One notable fact is that $\phi(\text{GCNL})$ is metal-dependent. This is because the major factors in determining $\phi(\text{GCNL})$ are metal band structures and metal dependent interface structures. Our estimated $\phi(\text{GCNL})$ on HfO₂ indicates a decrease in WFs of *n*-metals and an increase in WFs of *p*-metals. These changes in the WFs originate from the electron transfer due to interface hybridization between the metal and HfO₂ wave functions.

To confirm the validity of the $\phi(\text{GCNL})$ concept, we performed the XPS experiments using a metal nano-dot technique. The basic principle of the metal nano-dot technique is schematically illustrated in Fig. 14. The absolute value of the dipole at the interface between an electrically isolated metal nano-dot and an insulator is essentially smaller than that at the interface between a continuous metal and an insulator, although the interface dipole directions are the same. Thus, by comparing the core level shifts of these two interfaces, we can determine the interface dipole direction at a metal/insulator interface. Figure 15 shows the obtained Au-4*f* core level shifts of a Au nano-dot and continuous Au. As shown in Fig. 15, the measured Au 4*f* binding energies of continuous films are larger than those of electrically isolated nano-dots. These results clearly show the electron transfer from Au to HfO₂ at a Au/HfO₂ interface. Further, $\Delta V_{\text{fb,s}}$ obtained from CV curves indicate the electron transfer from Au(Ni) to HfAlO_x, and the transfer

from HfAlO_x to Al, respectively (Table I). These results coincide perfectly with the $\phi(\text{GCNL})$ prediction, and indicate the validity of our $\phi(\text{GCNL})$ concept.

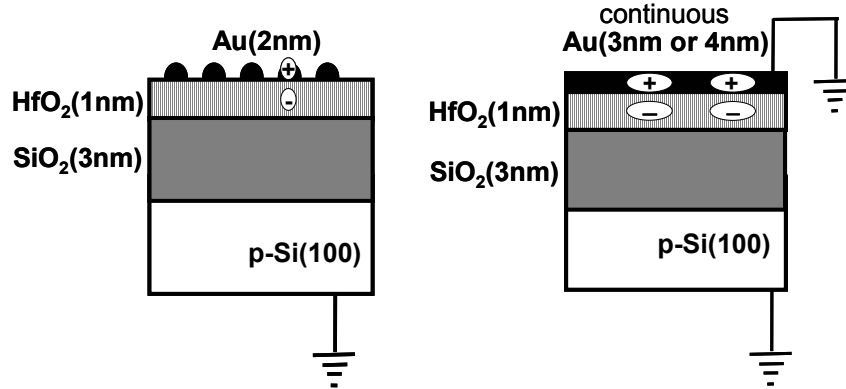


Fig.14: Schematic illustration of the basic principle of the metal nano-dot technique.

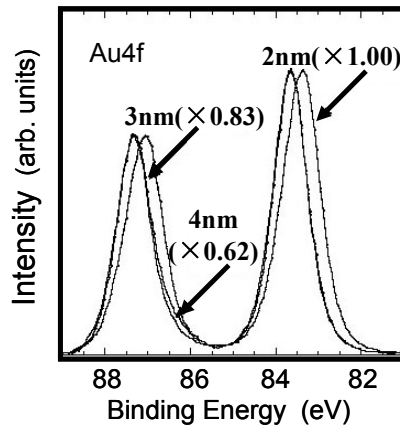


Fig.15: Au 4f spectra taken from the Au/HfO₂/SiO₂/Si gate stacks with varying Au dot sizes (2nm~4nm). The binding energy was calibrated with the Hf 4f 7/2 peak at 16.7eV and no energy shift in O 1s was detected.

Table I
Measured ΔV_{fb} of Al, Ni, and Au gates on HfAlO_x/SiO₂/Si stacks. ΔV_{fb} is obtained by subtracting the ideal CV curve from the measured CV curves with metal gates. The HfAlO_x thickness is 3nm.

	ΔV_{fb} (V)
Al	-0.35
Ni	0.20
Au	0.22

Guiding principles for achieving band edge work function metals and the potential of high-k La₂O₃ dielectrics

Based on our proposed concept $\phi(\text{GCNL})$, we can provide guiding principles for achieving band edge work function metals. For *n*-metals, a high-reactivity with O that induces a metal-O-Hf interface structure is desirable. On the other hand, for *p*-metals, metals that have characteristics of low reactivity with O that give rise to metal-Hf bonds and large occupied DOS are desirable, as schematically illustrated in Fig. 16.

Recently, a new high-k oxide La₂O₃, has attracted much attention for devices at the 32nm-node and beyond (3). Using the $\phi(\text{GCNL})$ concept, we examine the potential of La₂O₃ dielectrics. The cation content is larger in La₂O₃ than in HfO₂ due to the composition in the chemical formula. Thus, it is expected that the DOS of the La₂O₃ conduction bands is larger than that of the HfO₂ conduction bands. This will lead to an increase in interface hybridization between the metal occupied state wave functions and the La₂O₃ conduction band wave functions as illustrated in Fig. 17. Accordingly, a large electron transfer from metal to high-k oxide is expected in La₂O₃. In other words, the $\phi(\text{GCNL})$ concept simply predicts that higher work function metals are likely to be

obtained on high-k La_2O_3 dielectrics. Thus, La_2O_3 is expected to have an advantage over HfO_2 in obtaining p -like band edge work function metals. However, further more detailed considerations, which includes the stability of the interface structures and the strength of metal-La bonds, are necessary to achieve a more reliable prediction.

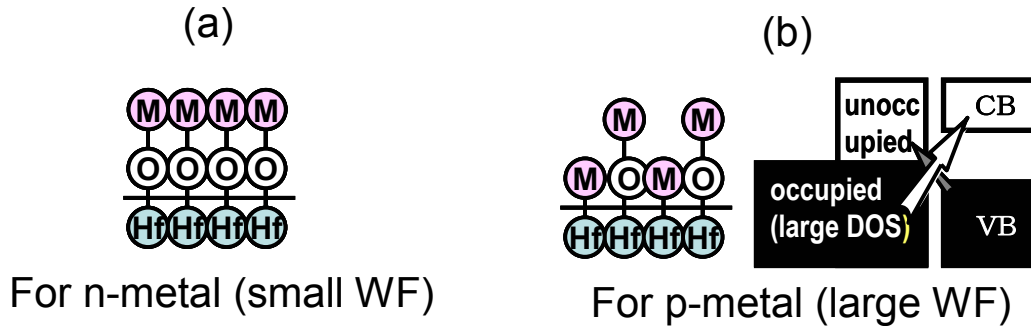


Fig.16: Schematic views of guiding principles for achieving n- and p- metals.

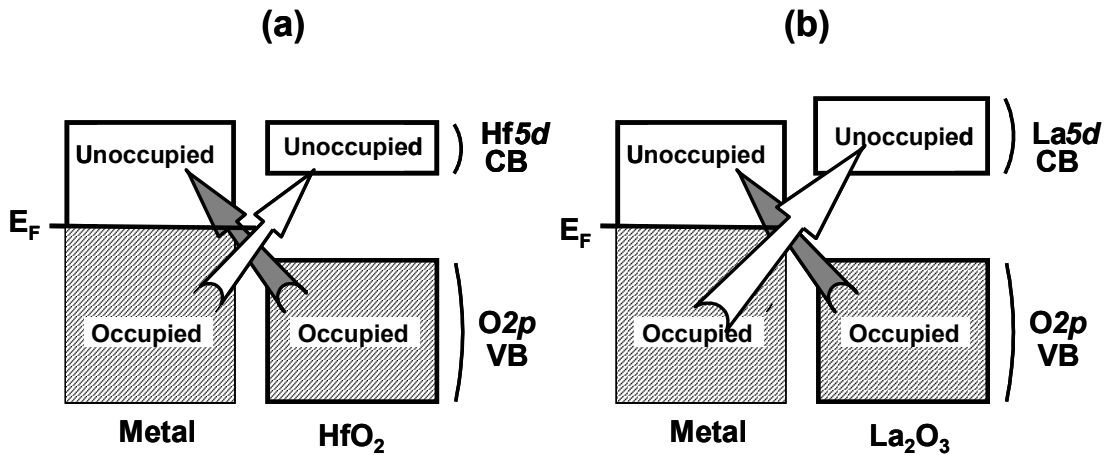


Fig.17: Schematic illustration of the comparison between the interface hybridization between metal occupied states and the high-k oxide conduction bands. (a) HfO_2 . (b) La_2O_3 .

Effective work functions of metal silicides

In this subsection, we show that effective the WFs of metal silicides can be predicted by our theory. The combination of $\phi(\text{GCNL})$ and V_o effects makes it feasible to discuss the curious WF behavior in Ni-rich Ni_xSi gates (5). Due to the presence of Si in Ni_xSi , the interface between Ni_xSi and a Hf-based dielectric is expected to be SiO_2 -like due to the partial oxidation of Si, in the thermal equilibrium condition. In this situation, V_o s are formed in HfO_2 causing Fermi level pinning (FLP), the same as in the case of poly-Si gates (10-12). In non-thermal equilibrium conditions, on the other hand, the remaining interfacial Ni-Hf bonds can lower the $\phi(\text{GCNL})$, and the FLP will be relaxed leading to an effective increase in the WF. To confirm this mechanism, we measured the Ni content and the annealing temperature dependence of the WFs of Ni_xSi on HfO_2 . Ni_xSi films were deposited by co-sputtering on the $\text{HfO}_2/\text{SiO}_2$ stack and on SiO_2 . All samples exhibit FLP after annealing at 800 °C, whereas, the FLP is relaxed in the Ni-rich Ni_xSi with decreasing annealing temperature (Fig. 18(a)). Further, the CV curve of the $\text{Ni}_{0.87}\text{Si}_{0.13}$ sample after an annealing at 450 °C exhibits clear humps (Fig. 18(b)). These

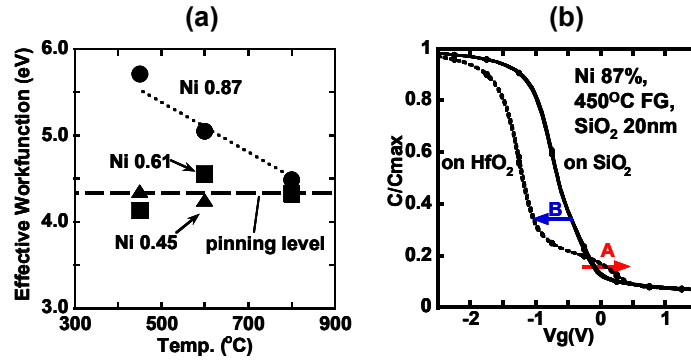


Fig. 18: (a) Effective WFs of Ni_xSi_{1-x} on HfO_2 plotted as functions of an annealing temperature. Ni contents (x) are 0.87, 0.61 and 0.45. (b) Measured CV curves of $Ni_{0.87}Si_{0.13}$ on HfO_2 after annealing at 450 °C. Clear humps, denoted by A and B, are observed.

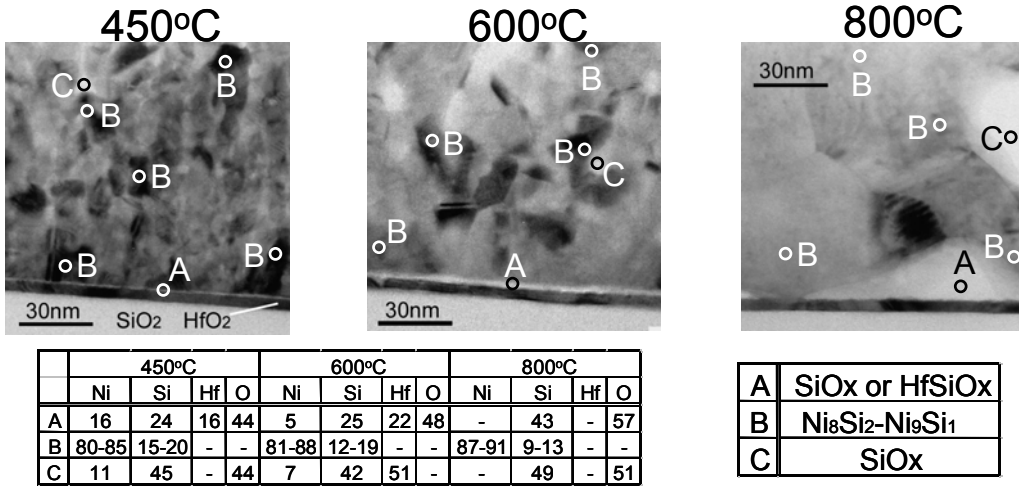


Fig. 19: Cross sectional TEM pictures of the $Ni_{0.87}Si_{0.13}$ electrodes annealed at 450, 600 and 800 °C. Chemical compositions determined from EDX (energy dispersive X-ray analysis) measurements are summarized in the Table.

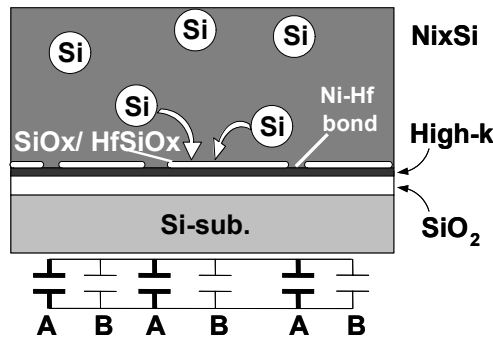


Fig. 20: Schematic illustration of the $Ni_{0.87}Si_{0.13}/HfO_2$ interface after a 450 °C-annealing. Formation of a discontinuous SiO_x or $HfSiO_x$ layer between gates and high-k dielectrics will result in the humps in the CV curve (Fig.18(b)), due to inhomogeneous effective WFs at the interface.

humps suggest the existence of two types of structure at the interface

To clarify the detailed interface structure, we performed TEM and EDX measurements. As shown in Fig. 19, the microscopic structures of the Ni_xSi electrodes can be categorized into three regions as summarized in the Table in Fig. 19; (A) an interfacial amorphous SiO_x or $HfSiO_x$ layer, (B) Ni-rich crystal grains and (C) amorphous SiO_x in the Ni_xSi . Growth of a thick interfacial oxide layer (A) was observed after annealing at 800 °C. Growth of such a thick interfacial oxide layer (A) should result in the FLP due to V_o generation (10-12). On the other hand, the thickness of the interfacial layer after annealing at 450 °C was less than 1nm. Thus, the interfacial layer (SiO_x or $HfSiO_x$) is discontinuous, and this causes the humps in the CV curve due to inhomogeneous effective WFs, as illustrated in Fig. 20. Moreover, the expected Ni-Hf bonds at the interface increases the effective WFs of $Ni_{0.87}Si_{0.13}$. This is a natural explanation why Ni-rich Ni_xSi after low temperature annealing has a large effective WF. Finally, we compare our proposed theory with other existing models in Fig. 21. It is clear that only our theory can perfectly explain the observed effective WFs of various gate materials on Hf-based high-k dielectrics.

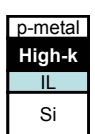
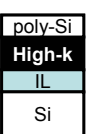
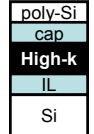
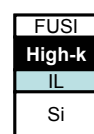
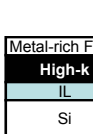
							
	n-metal	p-metal	poly-Si without cap layer	poly-Si with cap layer	FUSI without cap layer	FUSI with cap layer	Metal- rich FUSI
Hf-Si bonds [Ref. 6]	—	—	good	poor	good	poor	good
$\phi(CNL)$ [Ref. 7, 8, 9]	good	poor	poor	poor	poor	poor	poor
$\phi(GCNL)+V_o$ [This theory]	good	good	good	good	good	good	good

Fig. 21: The applicability of several models to explain the WF behavior of various gate materials on Hf-based high-k dielectrics.

CONCLUSION

We have proposed a new concept to determine the charge neutrality level of metal/Hf based high-k dielectrics, taking into account the facts that the MIGS penetration depth is only 1-2 atomic layers and the DOS of p -metal is not featureless, which make the conventional charge neutrality level concept inapplicable. It has been shown that the unusual behavior of WFs of Au, Ni, and Ni_xSi can naturally be explained using our newly proposed concept of $\phi(GCNL)$ and V_o . Using $\phi(GCNL)$, we show that there is the potential to obtain p -like band edge metals with the high-k dielectric La_2O_3 , since it is expected that the large hybridization between the metal occupied states and the La_2O_3 conduction bands can be obtained due to the expected large DOS of the La_2O_3 conduction bands. Moreover, our theory also predicts that control of the ratio of the interfacial bond number $N_{metal-Hf}/N_{metal-O-Hf}$, is crucial especially for tuning the WFs of p -metals, which is a practical guiding principle for the selection of the metal gate material.

References

- [1] G. D. Wilk and R. M. Wallace, *Appl. Phys. Lett.*, **74**, 2854 (1999).
- [2] G. D. Wilk, R. M. Wallace, J. M. Anthony, *J. Appl. Phys.*, **89**, 5243 (2001).
- [3] J. A. Ng, Y. Kuroki, N. Sugii, K. Kakushima, S.-I. Ohmi, K. Tsutsui, T. Hattori, H. Iwai, and H. Wong, *Microelectronic Engineering*, **80**, 206 (2005).
- [4] M. Koyama, Y. Kamimuta, T. Ino, A. Kaneko, S. Inumiya, K. Eguchi, M. Takayanagi, and A. Nishiyama, p.499, *Technical Digest of IEEE International Electron Devices Meeting, San Francisco, USA*, (2004).
- [5] M. Terai, K. Takahashi, K. Manabe, T. Hase, T. Ogura, M. Saitoh, T. Iwamoto, T. Tatsumi, and H. Watanabe, p.68, *Tech. Digest of 2005 Symposium on VLSI Technology, Kyoto, Japan*, (2005).
- [6] C. Hobbs, L. Fonseca, V. Dhandapani, S. Samavedam, B. Taylor, J. Grant, L. Dip, D. Triyoso, R. Hegde, D. Gilmer, R. Garcia, D. Roan, L. Lovejoy, R. Rai, L. Hebert, H. Tseng, B. White, and P. Tobin, p.9, *Technical Digest of 2003 Symposium on VLSI Technology, Kyoto, Japan*, (2003).
- [7] J. Tersoff, *Phys. Rev. Lett.*, **52**, 465 (1984).
- [8] M. Cardona and N. E. Christensen. *Phys. Rev. B*, **35**, 6182 (1987).
- [9] J. Robertson, *J. Vac. Sci. Technol. B*, **18**, 1785 (2000).
- [10] K. Shiraishi, K. Yamada, K. Torii, Y. Akasaka, K. Nakajima, M. Konno, T. Chikyo, H. Kitajima, and T. Arikado, p.108, *Technical Digest of 2004 Symposium on VLSI Technology, Honolulu, USA*, (2004).
- [11] K. Shiraishi, K. Yamada, K. Torii, Y. Akasaka, K. Nakajima, M. Konno, T. Chikyo, H. Kitajima, and T. Arikado, *Jpn. J. Appl. Phys. Part 2*, **43**, L1413 (2004).
- [12] H. Takeuchi, H-Y.Wong, D. Ha, and T-J. King, p.829, *Technical Digest of IEEE International Electron Devices Meeting, San Francisco, USA*, (2004).
- [13] E. Cartier, F.R. McFeely, V. Narayanan, P. Jamison, B. P. Linder, M. Copel, V. K. Pruchuri, V. S. Basker, R. Haight, D. Lim, R. Carruthers, T. Shaw, M. Steen, J. Sleight, J. Rubino, H. Deligianni, S. Guha, R. Jammy and G. Shahidi, p.230, *Tech. Digest of 2005 Symposium on VLSI Technology, Kyoto, Japan*, (2005).
- [14] K. Shiraishi, Y. Akasaka, S. Miyazaki, T. Nakayama, T. Nakaoka, G. Nakamura, K. Torii, H. Furutou, A. Ohta, P. Ahmet, K. Ohmori, H. Watanabe, T. Chikyow, M. L. Green, Y. Nara, and K. Yamada, p.43, *Technical Digest of IEEE International Electron Devices Meeting, Washington D.C., USA*, (2004).
- [15] S. G. Louie and M. L. Cohen, *Phys. Rev. B*, **13**, 2461 (1976).
- [16] W. Mönch, *Appl. Surf. Sci.*, **92**, 367 (1996).
- [17] Y. Akasaka₁, K. Miyagawa₁, A. Kariya₁, H. Shoji₁, T. Aoyama₁, S. Kume₁, M. Shigetani₁, O. Ogawa₁, K. Shiraishi, A. Uedono, K. Yamabe, T. Chikyow, K. Nakajima, M. Yasuhira₁, K. Yamada, and T. Arikado, p. 196, *Extended Abstracts of International Conference on Solid State Devices and Materials, Tokyo, Japan*, (2004).
- [18] J. P. Perdew, K. Burke, and M. Ernzerhof, *Phys. Rev. Lett.*, **77**, 3865 (1996).
- [19] D. Vanderbilt, *Phys. Rev. B*, **41**, 7892 (1990).
- [20] J. Yamauchi, M. Tsukada, S. Watanabe, and O. Sugino, *Phys. Rev. B*, **54**, 5586 (1996).
- [21] T. Nakaoka, K. Shiraishi, Y. Akasaka, T. Chikyow, K. Yamada, and Y. Nara, p.860, *Extended Abstracts of the 2004 Conference on Solid State Device and Materials, Kobe, Japan*, (2005).
- [22] T. Nakayama, *Physica B*, **191**, 16 (1993).